A Method For Subject-Specific Body Model Generation using Affine And Non-Linear Transformations

Leeor Alon[1,2], Cem M. Deniz[1,2], Giuseppe Carluccio[1,2], Mary Bruno[1], Daniel K. Sodickson[1,2], and Christopher C. Collins[1,2]
[1]*Department of Radiology, Bernard and Irene Schwartz Center for Biomedical Imaging, New York University School of Medicine, New York, NY, United States,*
[2]*Sackler Institute of Graduate Biomedical Sciences, New York University School of Medicine, New York, NY, United States*

INTRODUCTION: Global RF power deposition and local specific absorption rate (SAR) are metrics needed to ensure patient safety. Recent developments allow global RF power deposition to be monitored effectively in vivo for single or multiple transmit systems [1], however routine in-vivo local SAR estimation currently relies heavily on *a priori* simulations, where MRI coils are modeled next to one or more of several pre-existing human body models, such as those of the virtual family [2]. Typically, RF coils are driven with a current or voltage source and the resulting local SAR distribution is assessed, however, body models used are not routinely personalized to the geometry of the patient being scanned and geometrical inaccuracies associated with the body models have a significant effect on local SAR and temperature change (ΔT) distributions in the body [3]. Recently, a method for patient-specific estimation of SAR was proposed utilizing rapid acquired fat and water tissues content to produce a simplistic human body with a few tissue types [4]. Meanwhile, experimental techniques for electrical property mapping have attempted to map the in vivo electrical properties of patients scanned and estimate SAR [5,6], however, these measurements can be lengthy and SAR estimation for those is not yet feasible in the clinical setting. In this work, a method for the creation of body models that resemble the patient being scanned in orientation, geometry and tissue composition is presented. Affine and non-linear deformations were used to transform an image of a "source" along with his/her segmented conductivity, permittivity and density maps to that of a target subject's image, creating a patient-specific body mode. Preliminary results of the subject-specific transformation are shown for the head region of two different subjects.

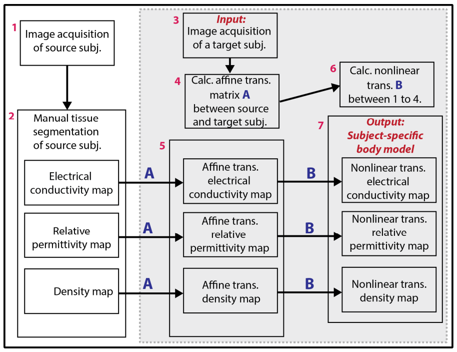

Figure 1. 1. Image acquisition of source subject. 2. The source subject is segmented manually yielding 3D electrical conductivity, relative permittivity and density maps. 3. A target subject is scanned. 4. An affine 12-paramemter affine transformation (denoted as A) between a source subject and a target subject is computed. 5. A is used to transform the source subject and the electrical conductivity, relative permittivity and density maps to resemble those of the target subject. 6. A non-linear transformation (denoted as B) is then calculated between the affine transformed source subject and the target subject for a finer transformation. 7. B is used to transform the affine transformed conductivity, permittivity and density maps to create subject-specific maps. Steps 4-7 in the grayed area were automated to for the transformation of random subjects

METHODS: A first ("source") subject was placed in a 3T Skyra Siemens scanner (Siemens Medical Solutions, Erlangen, Germany) and imaged using a 32 receive channel receive head coil. A 3D spoiled gradient echo MPRAGE turbo flash sequence was acquired with imaging parameters: TE=2.3, TR=2200, flip angle=9, TI=900, matrix size=256x256x192, IPAT=2, phase Fourier 7/8th, slice Fourier 7/8, voxel size=1x1x1mm^3 and total acquisition time= 4 minutes and 31 seconds. The reconstructed DICOM images of the source head were segmented by hand using MIPAV (National Institute of Health, Bethesda, MD). Eleven different tissues were used for the segmentation, including: Air, blood, bone, gray matter, white matter, cartilage, cerebrospinal fluid (CSF), eye, fat, skin and cerebellum, each of which was assigned an electric conductivity, relative permittivity and mass density according to ref [7]. Two different second ("target") subjects were then imaged in the same scanner and coil with similar imaging parameters and images of the subject's head were export to a computer. Using the Statistical Parameter Mapping (SPM) toolbox (Functional Imaging Laboratory, London, UK) for Matlab (Mathworks, Natick, MA), the 3D image of the head of the source subject was co-registered to each head image of the target subjects. Similar registration was applied to the electric conductivity, relative permittivity and mass density maps with coordinates corresponding to the source subjects'. After registration of the heads, a 12-parameter affine transformation matrix was calculated between the source and each of the target subjects' heads using least squares solution [8]. The affine transformation matrix was then used to transform the image of the source subject's head to the head of the target subject. Equivalent transformation was also applied to the conductivity, permittivity and density maps. The following parameters were used to estimate the affine transformation matrix: minimization function: least squares, resolution 1x1x1mm^3, and no regularization. After the source subject's head was co-registered and linearly transformed to the target subject's head, non-linear spatial transformation was applied such that the image of the source subject's head was nearly identical to the image of the head of the target subject [9]. For the non-linear transformation, the *spm_normalise* function was used and once the parameters of the non-linear transformation operation were calculated, the electrical conductivity, relative permittivity and mass density maps were transformed using these parameters. The following parameters were used for the non-linear transformation: template curve smoothing 5mm, DCT cutoff=15mm, iterations 50, and no regularization. The procedure (steps 3-7 in Fig 1) was automated in Matlab, and the transformation of the high-resolution images took approximately 15 minutes on a MacBook Air iCore 7 laptop with 8GB of ram. Once the computation and writing of the files concluded, images showing the transformations between the heads and errors were plotted.

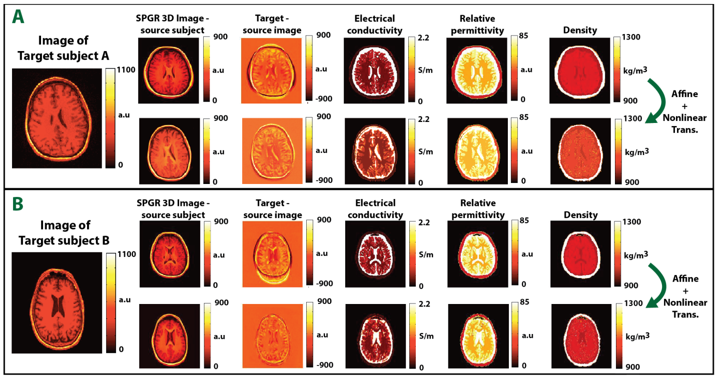

Figure 2. Transformation of a single source subject to two target subjects second subject was calculated based on affine and non-linear transformations. These transformations were used to deform the source subject's head (top row) to resemble the head of the second subject. After transformation (bottom row) the difference between the heads is minimized and the transformation was used to deform the electrical conductivity, relative permittivity and density maps.

RESULTS: Figure 2 shows the results of the transformations performed on the source subject's head such that it matches the head of two different random subjects (A and B). The top row of A and B illustrate the source subject's anatomy before transformation and the bottom row shows the anatomy post-transformation. The same transformations calculated were applied to the electrical conductivity, relative permittivity and density maps as shown in Figure 2A and B.

CONCLUSION: In summary, an automatic method for creation of subject-specific body models with numerous tissues is presented in this work. The method utilizes information from a previously segmented source head of a subject and performs affine and non-linear operations such that the source subject's head anatomy matches the anatomy of the target. Future investigations will include application of the method on a multitude of anatomies and improving the speed of the computation in hopes that the methodology (along with increasingly-fast field calculations) can be used for real-time patient-specific SAR prediction.

REFERENCES: [1] Zhu, Y., et al. (2012), System and SAR characterization in parallel RF transmission. Magn Reson Med, 67: 1367–1378. [2] Christ A., et al, The VirtualFamily--development of surface-based anatomical models of two adults and two children for dosimetric simulations, Phys Med Biol, 55 (2010), pp. N23-38. [3] Alon L., et al. Do constraints on |B1+| also constrain |E| and SAR in high field MR?, ISMRM, 2011, pp. P. 6913. [4] Homann H., et al., Toward individualized SAR models and in vivo validation, Magn Reson Med, 66 (2011), pp. 1767-76 [5] Katscher K., et al., Determination of electric conductivity and local SAR via B1 mapping, IEEE Trans Med Imaging, 28 (2009), pp. 1365-74 [6] Sodickson D.K., et al. Local Maxwell Tomography Using Transmit-Receive Coil Arrays for Contact-Free Mapping of Tissue Electrical Properties and Determination of Absolute RF Phase, ISMRM, 2012, pp. 387. [7] Gabriel S., et al., The dielectric properties of biological tissues: II. Measurements in the frequency range 10 Hz to 20 GHz, Phys. Med. Biol. 41 (1996), 2251-2269. [8] Friston K.J., et al. Spatial Registration and Normalization of Images. Human Brain Mapping 2:165-189, 1995 [9] J. Ashburner J., et al. Nonlinear Spatial Normalization using Basis Functions. Human Brain Mapping 7(4), 1999.